

Evaluation for Morphology of Regions Having Microtexture in Ti-6Al-4V Alloy Forging Products

Dr. Yoshinori ITO*¹ • Dr. Hiroyuki TAKAMATSU*² • Shogo SAEKI*³ • Dr. Nobuhiro TSUJI*⁴

*¹ Materials Research Laboratory, Technical Development Group

*² Digital Innovation Technology Center, Technical Development Group

*³ Takasago Quality Assurance Department, Advanced Materials Business

*⁴ Kyoto University Graduate School

Abstract

Titanium alloys contain regions having microtexture, in which the crystallographic orientation of the alpha phase is similar. Because the regions with microtexture deteriorate mechanical properties, it is important to evaluate their morphology. In this study, ultrasonic measurement was conducted, and the results were compared with characterization results obtained by the SEM/EBSD method. It has been verified that backscattered signals by ultrasonic measurement can be used for the evaluation of the regions having microtexture.

Introduction

Titanium alloys are used in aerospace industry thanks to their excellent specific strengths. Ti-6Al-4V is the most popular among titanium alloys. This alloy consists of α phase with hcp structure and β phase with bcc structure, and volume fraction of α phase is approximately 90 % at room temperature.^{1),2)}

The mechanical properties of titanium alloy depend on the microstructural morphology of α phase. In applications that require high fatigue strength and ductility, the α phase is controlled to be granular. The outline of the process is as follows. First, a lamellar type of α phase is formed by cooling from a high temperature region, in which β single phase is stable, to room temperature. Next, hot forging is conducted at a temperature where the two phases of $\alpha + \beta$ are stable to make the granular morphology of α . After that, solution heat treatment and aging heat treatment are performed in the $\alpha + \beta$ region as needed.

The size of α grains after hot forging, observed by an optical microscope, is as fine as approximately 10 to 20 μm . However, it is reported that α grains form microtexture with a similar crystal orientation over a range exceeding several hundred micrometers, and such regions are called macrozones or microtextured regions.³⁾⁻¹⁴⁾ This paper refers to these regions as "macrozones." Each macrozone behaves like one large crystal grain and is reported to deteriorate fatigue properties.^{3), 4)} Therefore, in order to provide titanium alloy forgings with excellent quality, it is important to evaluate the macrozone.

Macrozones are generally evaluated by the electron backscatter diffraction in scanning electron microscopes (SEM/EBSD).^{15), 16)} However, this method leads to destructive evaluation, and requires a long time for wide range measurements. For non-destructive evaluation, studies are conducted using ultrasonic waves^{11), 12)}, but they are limited to cross-sectional evaluations.

Macrozones (a metallographic structure in a broad sense) are said to affect the scattering behavior of ultrasonic waves. In a study using a Ti-5Al-6V-2Sn alloy forging, Ginty et al. reported that maximum intensity of backscattered signal (the signal of ultrasonic waves that scatter in the direction opposite to the incident direction) is obtained when ultrasonic wave incident in a vertical direction of flat grain boundaries in a macrostructure.¹⁷⁾

Humbert et al. observed the microstructure of an IMI834 alloy forging having a great number of macrozones whose morphologies are long and arranged in parallel to each other, and showed that a large amplitude of backscattering is obtained when an ultrasonic wave incident in the vertical to the extended direction.⁷⁾ They discussed the reasons that the arrangement of the localized microtextures causes a pseudo-periodic fluctuation of crystal orientation (corresponding to the fluctuation of the elastic modulus described later). However, there are many unclear points about the quantitative effect of localized microtextures on the backscattering behavior of ultrasonic waves.

Hence, Kobe Steel evaluated the morphology of macrozones and its effect on the backscattering behavior of ultrasonic waves in cylindrical material of Ti-6Al-4V alloy.¹⁸⁾ The results showed that macrozones elongated in the longitudinal direction were formed and that anisotropy of the amplitude of the backscattered signals was exhibited, which depended on the incident direction of the ultrasonic wave. Moreover, this anisotropy has been shown to be explained by the fluctuation of the elastic modulus caused by macrozones.

The present study conducted a further investigation of the previous study.¹⁸⁾ Hence, its purpose is to clarify the effects of the incident direction and incident angle of ultrasonic wave

on the amplitude of backscattered signals and to evaluate a three-dimensional morphology of macrozones. The subject material is a Ti-6Al-4V alloy forging, which has been cogged into a cylindrical shape in the $\alpha + \beta$ phase region and has a granular morphology of α .

1. Experimental method

1.1 Preparation of test material

The test material is Ti-6Al-4V alloy. The lowest temperature in the β single phase region (β transus) is 988 °C. A columnar material having a diameter of 405 mm was heated and held in the β monophasic region and then water-cooled. After the oxidation scale on the surface had been removed, cogging and upset forging were performed multiple times in the hot temperature range of $\alpha + \beta$ to obtain a columnar material with a diameter of 165 mm. The forged material was air-cooled to room temperature. Specimens were cut out from this columnar material and used for the evaluation. Fig. 1 shows the specimen position in forged material and its coordinate system. Hereinafter, the plane vertical to the tangential direction (TD) of the columnar material will be referred to as the "longitudinal section," and the plane vertical to the axial direction (AD) will be referred to as the "transverse section."

1.2 Microstructure of columnar material and SEM/EBSD measurements

The optical micrograph observed for the longitudinal section of the columnar material is shown in Fig. 2.¹⁸⁾ In this figure, the gray regions, each observed in the form of a lump, are granular α , which occupies the most region of the microstructure. Although it is difficult to distinguish from the photograph of this magnification, in space of granular α , there exist

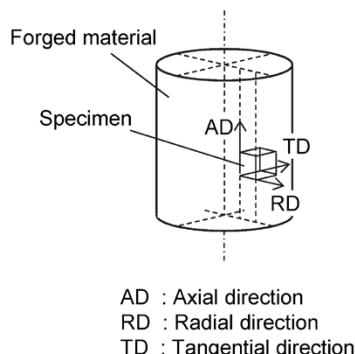


Fig. 1 Schematic illustration of specimen position in forged material and coordinate system

small colonies which consist of a plate-shaped α phase and a residual β phase.

In this study, electron backscatter diffraction (EBSD) measurement was performed in a scanning electron microscope (SEM) to evaluate the macrozone. At that time, in order to evaluate the three-dimensional morphology, the longitudinal section and the transverse section were evaluated, respectively.

1.3 Ultrasonic measurement

The shape of the specimen is a cuboid with lengths in the radial direction (RD), axial direction (AD), and tangential direction (TD) of 52 mm, 35 mm, and 57 mm, respectively. A frequency of 10 MHz was used for the ultrasonic measurement. The wavelength that propagates through the titanium alloy is approximately 600 μm . A flat probe was immersed in water with the specimen, an ultrasonic wave was sent from the probe, and a backscattered signal from inside the material was received by the same probe. The transmitted ultrasonic wave was a pulsed plane wave. The incident wave was transmitted in 2 directions in the RD and AD of the columnar material. For the measurement in the RD, the incident angle was tilted with reference to the RD (0°). The probe was tilted along two directions, a direction parallel to the AD and a direction parallel to the TD. Measurements were performed with angles tilted at a pitch of 1° in the range of -4° to +4°. The backscattered signal was amplified with a gain of 40 dB to make sufficient signal strength for analysis. The strength of the backscattered signal, generated when the ultrasonic wave propagated inside the material, was averaged with respect to the depth direction of the material and was used for the analysis. Hereinafter, this averaged value will be referred to as the "backscattered signal strength."

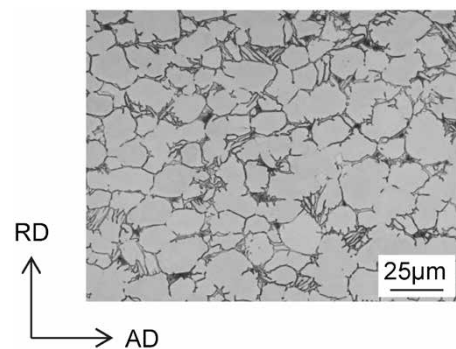


Fig. 2 Optical microstructure of Ti-6Al-4V material forged in $\alpha + \beta$ phase region¹⁸⁾

1.4 Basic principle of ultrasonic measurement

The ultrasonic wave propagates in a material and scatters at the interface of two regions with different acoustic impedances. The acoustic impedance is expressed by Equations (1) and (2).

$$Z = \sqrt{\rho \cdot V_L} \quad \dots\dots\dots (1)$$

$$V_L = \sqrt{C/\rho} \quad \dots\dots\dots (2)$$

wherein Z is the acoustic impedance, ρ is the density of the material, C is the elastic modulus of the material, and V_L is the acoustic velocity of the vertical wave.

The density inside a material is regarded to be homogeneous, and if the material has inside it an inhomogeneous microstructure whose elastic modulus is different from that of the surroundings, scattering occurs at the interface.

The main phase of Ti-6Al-4V alloy is α phase, and this paper focuses on the elastic modulus of α phase. The elastic constants, C_{11} , C_{33} , C_{12} , C_{13} , and C_{44} of an α -phase titanium single crystal consisting of hcp lattice are reported to be 162.4 GPa, 180.7 GPa, 92.0 GPa, 69.0 GPa and 46.7 GPa, respectively.¹⁹⁾ Here, C_{11} and C_{33} are elastic constants in the direction vertical to the c axis of the hcp lattice and in the direction parallel to the c axis, respectively. Because of the symmetry of the hcp lattice, the elastic modulus depends on the angle θ formed by the c axis with respect to the direction of stress loading and is equivalent around the c axis. The change in the elastic modulus with θ is shown in Fig. 3.¹⁸⁾ Thus, the change in crystal orientation accompanies the change in elastic modulus, which causes the scattering of ultrasonic waves. That is, the existence of macrozones is envisaged to cause the scattering of ultrasonic waves.

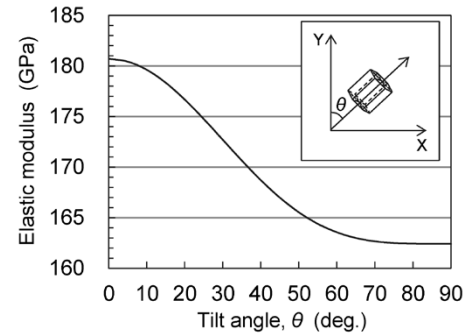


Fig. 3 Relationship between elastic modulus and tilt angle of c -axis in hcp lattice (α phase)¹⁸⁾

2. Experimental results and discussion

2.1 Morphology of macrozone

Fig. 4 shows the inverse pole figure orientation maps (IPF maps) obtained by SEM / EBSD.^{15), 16), 20)} Fig. 4 (a) is the measurement result in the longitudinal section, and Fig. 4 (b) is the measurement result in the transverse section. The coloring of each IPF map has been based on the standard triangle shown in the figure and shows the crystal orientation in the RD of respective measurement point. Fig. 5 (A) to (H) are (0001) pole figures^{15), 16), 20)} of the α phase in the regions A to H shown by the white rectangle frame in Fig. 4 (a).

First, the focus is on the IPF map of the longitudinal section (Fig. 4 (a)). Macrozones are found to be formed extending in the axial direction. Their thickness is several hundred μm and their length exceeds 1 mm. Under the optical microscope, a microstructure of granular α with a diameter of about 20 μm is observed (Fig. 2), while the results of SEM / EBSD measurement show that many adjacent α grains have a similar crystal orientation. Macrozones are also observed in the transverse

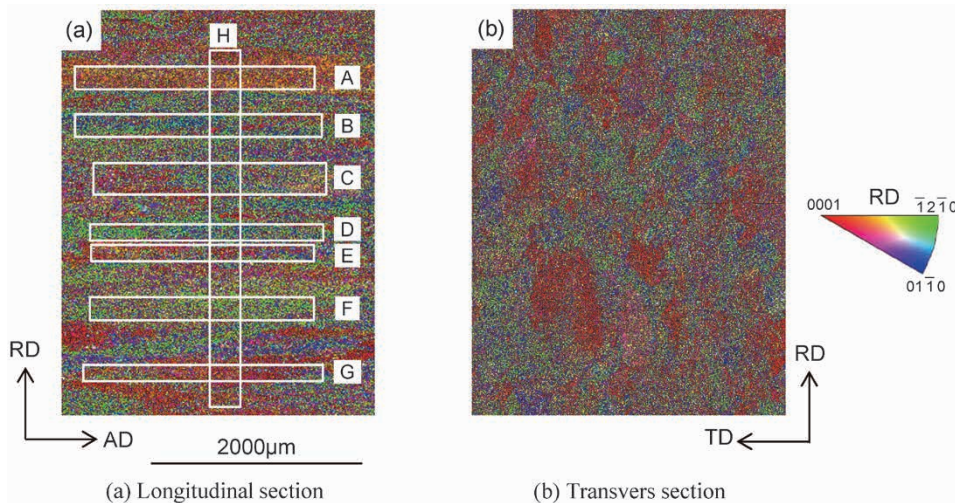


Fig. 4 EBSD IPF maps of Ti-6Al-4V material forged in $\alpha + \beta$ phase field

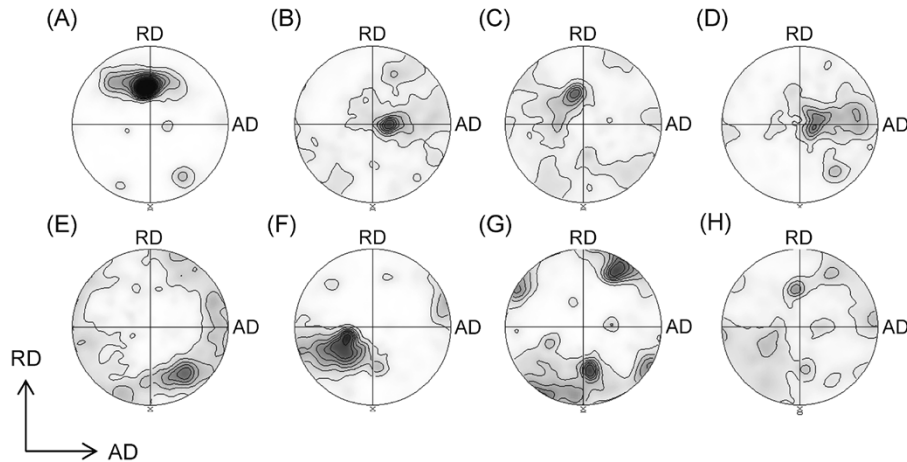


Fig. 5 (0001) pole figures of α phase in region A through H shown in Fig.4(a)

section (Fig. 4 (b)), but unlike the longitudinal section, they are almost equiaxial in shape. That is, it has been clarified that fibrous macrozones has been formed in the columnar material of the Ti-6Al-4V alloy used in this study.

In order to examine the features of the macrozones recognized in the longitudinal section in detail, the crystal orientation information in the frame indicated by the white rectangle in the figure has been organized in the format of pole figures^{15), 16), 20)} (Fig. 5). The regions A to G lie such that the long side of each rectangle is parallel to the axial direction (AD) of the columnar material, while region H lies such that the long side of the rectangle is parallel to the radial direction (RD). In the region A (Fig. 5 (A)), a strong texture of c-axis is observed in the orientation tilted from the TD to RD. This indicates that the region surrounded by each white rectangle in the IPF map of Fig. 4 (a) can be regarded as if it were a single crystal grain, as expected from the fact that each measurement point is mainly displayed in red or yellow. Similarly, in Fig. 5 (B) to (F), the c-axes are tilted in almost one orientation. However, the orientations of texture are different from each other. For example, in the region B (Fig. 5 (B)) adjacent to the region A, almost all c-axes are tilted in the orientation close to the TD, unlike the region A. The region C (Fig. 5 (C)) and the region D (Fig. 5 (D)) show strong texture in orientations close to the region A and the region B, respectively. In the region E (Fig. 5 (E)) and the region F (Fig. 5 (F)), the observed textures are different from those of the regions A to D. In the region E, relatively high intensity of the c-axes is observed near the opposite side of the RD near the circumference of the pole figure. In the region F (Fig. 5 (F)), relatively high intensity of the c-axis is observed in the vicinity of the orientation tilted parallel from the TD to AD. In the region G (Fig. 5 (G)), unlike the regions A to E,

there are approximately three locations at which the intensity of the c-axis is relatively high. As shown in Fig. 3, the elastic modulus of the α phase changes depending on the angle θ . The results of Fig. 4 (a) and Fig. 5 (A)-(G) suggest that a large number of macrozones extending in the AD are formed in the columnar material of Ti-6Al-4V alloy and, due to the difference in crystal orientation (formed angle θ) in each region, the elastic modulus changes at a pitch of several hundred μm along the RD. On the other hand, strong texture isn't found in the region H (Fig. 5 (H)), in which the long sides of the region, from which the crystal orientation information is extracted, matches the RD, and the degree of texture intensity is small compared with the regions A to G. The IPF map in Fig. 4 (a) is considered to indicate that, if the long side of the rectangle matches the RD, the region contains multiple macrozones and shows no strong texture.

As described above, the columnar material of Ti-6Al-4V alloy forged in the $\alpha + \beta$ region has long fibrous macrozones extending in the AD and their crystal orientations (θ) are different from each other. It is considered that this difference has caused the fluctuation of the elastic modulus along the RD. On the other hand, the texture of crystal orientation in the region in the vertical direction is not remarkable, suggesting that the fluctuation of the elastic modulus along the AD is small.

2.2 Strength of backscattered signal obtained by ultrasonic measurement

Fig. 6 shows the strength of the backscattered signal obtained when the columnar material is measured parallel to the RD and AD. Similar to the results of the previous study,¹⁸⁾ the backscattered signal strength is greater when measured in the RD than when measured in the AD, showing an

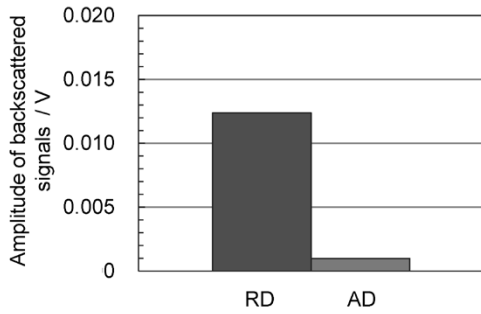


Fig. 6 Amplitude of backscattered signals obtained in RD and AD in ultrasonic measurements on Ti-6Al-4V material forged in $\alpha + \beta$ phase region

anisotropy depending on the measurement direction. In a forging of near α -type titanium alloy, it has been pointed out that the periodic fluctuation of the elastic modulus causes the backscattering of ultrasonic wave.⁷⁾ As shown in the previous section, the columnar material of Ti-6Al-4V alloy used in this study has a macrozone extending in the AD. Although the periodicity has not been evaluated in this study, the fluctuation of the elastic modulus is observed along the RD, in which the pitch of the fluctuation is several hundred μm and is close to the wavelength of the ultrasonic wave. On the other hand, no fluctuation of the elastic modulus is considered to occur along the AD. Therefore, the anisotropy of the backscattered signal strength observed in this study is also considered to be due to the presence or absence of variation in the elastic modulus in the measurement direction. In other words, the backscattering behavior can be said to change reflecting the morphology of the macrozone.

Focusing on the fact that the strength of the backscattered signal of the ultrasonic wave changes depending on the morphology of the macrozone, a study has been conducted on the utilization of the macrozone for morphological evaluation. Fig. 7 shows the results of study on the changes in the strength of the backscattered signal by tilting the incident angle in the range from -4° to $+4^\circ$ for the measurement in the RD. Fig. 7 (a) shows the results when the tilt is along the AD, and Fig. 7 (b) shows the results when it is along the TD. The zero degree on the horizontal axis indicates that an ultrasonic wave has been sent in parallel with the RD. From Fig. 7 (a), it can be seen that the change in the strength of the backscattered signal is greater when the tilt is made along the AD. The maximum backscattered signal strength is reached at the tilt angle of 1° , and the strength drops sharply regardless of whether the tilt is made in either the positive or negative direction. On the other hand, as shown in Fig. 7 (b), there is almost no change in the strength of the backscattered signal when the tilt is

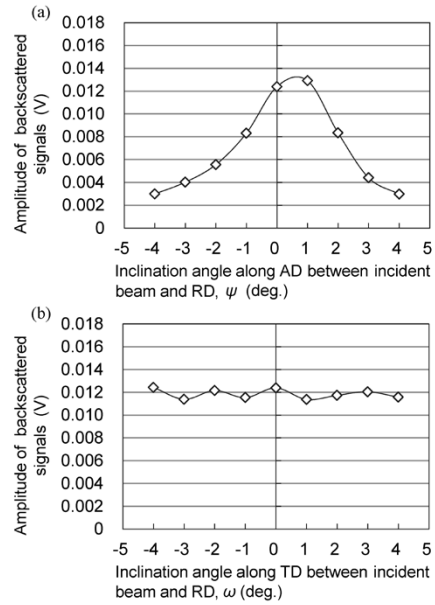


Fig. 7 Influence of incident angles and inclination direction on the amplitude of backscattered signals ((a) inclined along AD, (b) along TD)

made along the TD. Thus, it has been clarified that the strength of the backscattered signal responds sensitively to the incident angle, and that the change in the strength of the backscattered signal due to the incident angle greatly depends on the tilt direction.

This behavior is considered to be caused by the morphology of the macrozones formed in the columnar material of Ti-6Al-4V alloy. Since this study has investigated the fibrous macrozones extending in the AD, the interface of the macrozones has been formed in parallel to the AD. When ultrasonic wave propagates along the RD, elastic modulus fluctuations are caused by the macrozones, resulting in a backscattered signal with strong intensity. When the incident angle is tilted along the AD, however, the angle between the interface of the macrozone and the incident direction changes accordingly, resulting in slow fluctuations of the elastic modulus along the propagation direction of the ultrasonic wave. This is considered to have caused the sharp drop in the strength of the backscattered signal. It should be noted that the reason for the maximum strength of the backscattered signal being measured at the tilt angle of 1° is presumed that the extension direction of the macrozone is not perfectly parallel to the AD but is slightly slanted.

On the other hand, when the incident angle is tilted along the TD, almost no change occurs in the strength of the backscattered signal. The macrozones are fibrous and have a curved interface in the TD. In addition, the tilt along the TD does not change the relationship between the macrozone

and the extension direction. Therefore, it is considered that the change in the variation of the elastic modulus at the incident angle is small, hardly changing the strength of the backscattered signal.

As described above, it has become clear that the strength of the backscattered signal obtained by ultrasonically measuring the columnar material of Ti-6Al-4V alloy is sensitively affected by the incident direction and incident angle, and its behavior is affected by the morphology of the macrozone.

Conclusions

This study has shown that the strength of the backscattered signal of the ultrasonic wave depends on the morphology of the macrozone formed in titanium alloy forgings and changes sensitively depending on its incident direction and incident angle. This phenomenon can be exploited in the morphological evaluation of macrozones by ultrasonic waves. The morphology of the macrozones dealt with in this study are fibrous, however, there may be other morphologies such as pancake-shaped or oval-shaped. It is believed that a more universal morphological evaluation technology can be established by performing similar evaluations on these morphologies. It is considered that the spatial distribution of macrozones also affect the mechanical properties, and further studies will be conducted in the future.

References

- 1) J. W. Elmer et al. *Materials Science and Engineering A*. 2005, Vol.391, pp.104-113.
- 2) S. Kar et al. *Metallurgical and Materials Transaction A*. 2006, Vol.37, pp.559-566.
- 3) A. P. Woodfield et al. *Titanium 95 Science and Technology*. 1995, pp.1116-1123.
- 4) K. Le Biavant et al. *Fatigue & Fracture of Engineering Materials & Structures*. 2002, Vol.25, pp.527-545.
- 5) L. Germain et al. *Acta Materialia*. 2005, Vol.53, pp.3535-3543.
- 6) L. Germain et al. *Acta Materialia*. 2008, Vol.56, pp.4298-4308.
- 7) M. Humbert et al. *Acta Materialia*. 2009, Vol.57, pp.708-714.
- 8) R. Whittaker et al. *Materials Science and Technology*, 2010, Vol.26, pp.676-684.
- 9) L. Toubal et al. *Metallurgical and Materials Transaction A*. 2010, Vol.41, pp.744-750.
- 10) N. Gey et al. *Acta Materialia*. 2012, Vol.60, pp.2647-2655.
- 11) A. Moreau et al. *Materials Characterization*. 2013, Vol.75, pp.115-128.
- 12) A. L. Pilchak et al. *Metallurgical and Materials Transaction A*. 2014, Vol.45A, pp.4679-4697.
- 13) C. Buirette et al. *Materials Science and Engineering A*. 2014, Vol.A618, pp.546-557.
- 14) S. L. Semiatin. *Metallurgical and Materials Transaction A*. 2020, Vol.51A, pp.2593-2625.
- 15) S. Suzuki. *Materia Japan*. 2001, Vol.40, pp.612-616.
- 16) R. Yoda. *Compendium of Surface and Interface Analysis*, The Surface Science Society of Japan (ed.). Springer, 2018, pp.127-132.
- 17) B. Ginty et al. *Proceedings of the 14th World Conference on Titanium*. 2020., 11021. pp.1-4.
- 18) Y. Ito et al. *MATEC Web Conferences*. 2020, Vol.321, p. 11021.
- 19) E. S. Fisher et al. *Physical Review*. 1964, Vol.135, pp.482-494.
- 20) Y. Inagaki et al. *Journal of Japan Institute of Light Metals*. 2002, Vol.52, pp.494-499.